Available online at www.sciencedirect.com
SCIENCE DIRECT®
Journal of Sound and Vibration 293 (2006) 286–298
JOURNAL OF SOUND AND VIBRATION
www.elsevier.com/locate/jsvi

Micro-actuation characteristics of rocket conical shell sections

W.K. Chai[a], Y. Han[a], K. Higuchi[b], H.S. Tzou[a,*]

[a]*StrucTronics Lab, Department of Mechanical Engineering, University of Kentucky, Lexington, KY 40506-0503, USA*
[b]*Institute of Space and Astronautical Science, Kanagawa, Japan*

Received 30 October 2003; received in revised form 19 August 2005; accepted 29 September 2005
Available online 14 November 2005

Abstract

Rocket fairings, load-carrying structures of solid rocket motor case, e.g., inter-stage joint, satellite-rocket joint, etc., usually take the shape of conical shell sections. This paper is to evaluate spatially distributed microscopic control characteristics of distributed actuator patches bonded on conical shell surfaces. The converse effect of piezoelectric materials has been recognized as one of the best electromechanical effects for precision distributed control applications. The resultant control forces and micro-control actions induced by the distributed actuators depend on applied voltages, geometrical (e.g., spatial segmentation and shape) and material (i.e., various actuator materials) properties. Mathematical models and modal domain governing equations of the conical shell section laminated with distributed actuator patches are presented first, followed by formulations of distributed control forces and micro-control actions which can be divided into longitudinal/circumferential membrane and bending control components. Spatially distributed electromechanical microscopic actuation characteristics and control effects resulting from various longitudinal/circumferential actions of actuator patches are evaluated.

1. Introduction

Conical shell has a large load-carrying capacity per unit weight due to its high-strength, high-rigidity and light-weight properties. Conical shells and components are commonly found in structures of many vehicular/machine applications, such as nozzles, injectors, rocket fairings, and turbine engines. Effective distributed control of the conical shell section can enhance its performance, accuracy, precision and reliability. Free vibration analysis and flexural vibrations of conical shells with free edges were studied by Hu et al. [1,2]. Krause investigated natural frequencies and vibration characteristics of truncated conical shells with free edges [3]. Tong examined the effect of axial load on free vibration of orthotropic truncated conical shells [4]. The vibration characteristics of shallow conical shell were studied extensively by Liew et al. [5–7]. Recent development of smart materials further advances distributed actuation technologies that can be spatially laminated over structures [8]. Distributed control of conical shell laminated with full and diagonal actuators was investigated [9]. Active control of functionally graded-material cylindrical shells utilizing piezoelectric sensor/actuator patches was also investigated [10]. In addition, distributed control of paraboloidal shells was

*Corresponding author. Tel.: +1 (859)257 6336; fax: +1 (859)257 3304.
E-mail address: hstzou@engr.uky.edu (H.S. Tzou).

0022-460X/$ - see front matter © 2005 Elsevier Ltd. All rights reserved.
doi:10.1016/j.jsv.2005.09.017

also studied [11]. Moreover, distributed sensing of linear structures using distributed artificial neurons [12], and distributed sensing of linear [13] and nonlinear conical shells [14] or conical shell section has been investigated recently. This study focuses on dynamic distributed control and microscopic control actions of conical shell sections laminated with segmented piezoelectric actuator patches. Mathematical models and modal domain governing equations of the conical shell section laminated with distributed actuator patches are presented first, followed by formulations of distributed control forces and micro-control actions which can be divided into longitudinal/circumferential membrane and bending control components. Spatially distributed electromechanical microscopic actuation characteristics and control effects resulting from various longitudinal/circumferential actions are evaluated.

2. Control of conical shells with distributed actuators

A conical shell structure laminated with piezoelectric actuator layers is illustrated in Fig. 1 where x denotes the longitudinal direction, ψ the circumferential direction, and 3 the transverse direction. The geometric parameters of a conical shell are: the Lamé parameters $A_1 = 1$ and $A_2 = x \sin \beta^*$, the radii of curvature $R_1 = \infty$ and $R_2 = x \tan \beta^*$ where β^* is one-half of the apex angle. Independent modal control of conical shells with distributed piezoelectric actuators is discussed in this section. Micro-control actions and their directional control characteristics induced by actuator patches are discussed in the next section.

The modal expansion concept implies that the total response of the conical shell is composed of all participating modes. Thus, independent modal control characteristic of conical shells can be independently defined for each natural mode, considered there is no spillover and modal coupling:

$$\ddot{\eta}_m + 2\varsigma_m \omega_m \dot{\eta}_m + \omega_m^2 \eta_m = F_m, \tag{1}$$

where $\eta_m(t)$ is the modal participation factor, ς_m the modal damping ratio, ω_m the natural frequency, F_m the modal force, and the subscript m denotes the mth mode. The generic modal force F_m of the conical shell structure consists of two primary components: (1) the mechanical force induced by an external load F_i and (2)

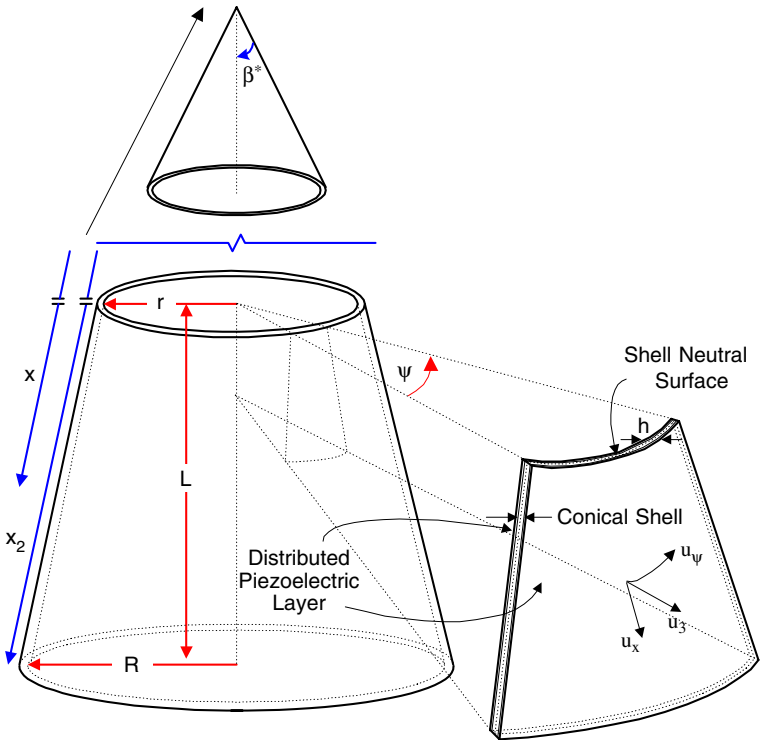

Fig. 1. A conical shell section and its coordinate system.

the control force induced by the distributed actuators $L_i^c(\phi_3)$ with a transversely applied electric control signal ϕ_3 (in *italic*):

$$F_m = \frac{1}{\rho h N_m}\int_{\alpha_1}\int_{\alpha_2}\left\{\sum_{i=1}^{3}[F_i + L_i^c(\phi_3)]U_{i_m}\right\}A_1A_2\,\mathrm{d}\alpha_1\,\mathrm{d}\alpha_2 = \hat{F}_m + \hat{F}_m^c, \tag{2}$$

where ρ is the shell mass density, h is the shell thickness, A_1 and A_2 are the Lamé parameters, α_1 and α_2, respectively, denote the x and ψ directions:

$$\hat{F}_m = \frac{1}{\rho h N_m}\int_{\alpha_1}\int_{\alpha_2}\left\{\sum_{i=1}^{3}F_iU_{i_m}\right\}A_1A_2\,\mathrm{d}\alpha_1\,\mathrm{d}\alpha_2,$$

$$\hat{F}_m^c = \frac{1}{\rho h N_m}\int_{\alpha_1}\int_{\alpha_2}\left\{\sum_{i=1}^{3}L_i^c(\phi_3)U_{i_m}\right\}A_1A_2\,\mathrm{d}\alpha_1\,\mathrm{d}\alpha_2$$

and

$$N_m = \int_{\alpha_1}\int_{\alpha_2}\left(\sum_{i=1}^{3}U_{i_m}^2\right)A_1A_2\,\mathrm{d}\alpha_1\,\mathrm{d}\alpha_2.$$

(Note that *italic* ϕ_3 denotes the control signal used in control action analysis presented later). $L_i^c(\phi_3)$ is Love's control operator induced by the converse piezoelectric effects and only a transverse applied voltage ϕ_3 is considered. The subscript i denote the coordinate directions, i.e., x, ψ and 3. The generic control operators imposed to a generic double-curvature shell in three directions are contributed by membrane control forces N_{ij}^c and counteracting control moments M_{ij}^c [15]:

$$L_1^c\{\phi_3\} = -\frac{1}{A_1A_2}\left\{\frac{\partial}{\partial\alpha_1}(N_{11}^cA_2) - N_{22}^c\frac{\partial}{\partial\alpha_1}A_2 + \frac{1}{R_1}\left[\frac{\partial}{\partial\alpha_1}(M_{11}^cA_2) - M_{22}^c\frac{\partial}{\partial\alpha_1}A_2\right]\right\}, \tag{3}$$

$$L_2^c\{\phi_3\} = -\frac{1}{A_1A_2}\left\{\frac{\partial}{\partial\alpha_2}(N_{22}^cA_1) - N_{11}^c\frac{\partial}{\partial\alpha_2}A_1 + \frac{1}{R_2}\left[\frac{\partial}{\partial\alpha_2}(M_{22}^cA_1) - M_{11}^c\frac{\partial}{\partial\alpha_2}A_1\right]\right\}, \tag{4}$$

$$\begin{aligned}L_3^c\{\phi_3\} = &-\frac{1}{A_1A_2}\left\{\frac{\partial}{\partial\alpha_1}\left(\frac{1}{A_1}\frac{\partial(M_{11}^cA_2)}{\partial\alpha_1} - \frac{M_{22}^c}{A_1}\frac{\partial A_2}{\partial\alpha_1}\right)\right.\\ &\left.+\frac{\partial}{\partial\alpha_2}\left(\frac{1}{A_2}\frac{\partial(M_{22}^cA_1)}{\partial\alpha_2} - \frac{M_{11}^c}{A_2}\frac{\partial A_1}{\partial\alpha_2}\right) - A_1A_2\left(\frac{N_{11}^c}{R_1} + \frac{N_{22}^c}{R_2}\right)\right\}.\end{aligned} \tag{5}$$

Substituting the Lamé parameters (i.e., $A_1 = 1$ and $A_2 = x\sin\beta^*$), radii of curvature (i.e., $R_1 = \infty$ and $R_2 = x\tan\beta^*$) and the two principal directions $\alpha_1 = x$, $\alpha_2 = \psi$ of the conical shell into the generic control forces yields Love's control operators of conical shells:

$$L_x^c\{\phi_3\} = -\left\{\frac{\partial N_{xx}^c}{\partial x} + \frac{1}{x}(N_{xx}^c - N_{\psi\psi}^c)\right\}, \tag{6}$$

$$L_\psi^c\{\phi_3\} = -\frac{1}{x\sin\beta^*}\left\{\frac{\partial N_{\psi\psi}^c}{\partial\psi} + \frac{1}{x\tan\beta^*}\frac{\partial M_{\psi\psi}^c}{\partial\psi}\right\}, \tag{7}$$

$$L_3^c\{\phi_3\} = -\left\{\frac{2}{x}\frac{\partial M_{xx}^c}{\partial x} + \frac{\partial^2 M_{xx}^c}{\partial x^2} - \frac{1}{x}\frac{\partial M_{\psi\psi}^c}{\partial x} + \frac{1}{x^2\sin^2\beta^*}\frac{\partial^2 M_{\psi\psi}^c}{\partial\psi^2} - \frac{N_{\psi\psi}^c}{x\tan\beta^*}\right\}. \tag{8}$$

The mode shape functions of the conical shell section with free boundary condition at both major and minor ends are based on the Donnell–Mushtari–Vlasov theory [3,9]. Thus, these mode shape functions are

expressed as

$$U_{xm} = U_{xm}(x)\cos(m\psi)\sin\,\omega_m t, \tag{9}$$

$$U_{\psi m} = U_{\psi m}(x)\sin(m\psi)\sin\,\omega_m t, \tag{10}$$

$$U_{3m} = U_{3m}(x)\cos(m\psi)\sin\,\omega_m t, \tag{11}$$

where m is the circumferential wavenumber and $m = 2\ldots\infty$; ω_m is the natural frequency. $U_{xm}(x)$, $U_{\psi m}(x)$ and $U_{3m}(x)$ are arbitrary displacement functions of x, satisfying the free–free displacement boundary conditions and they are selected as $(x/x_2)^p$ where p denotes the longitudinal mode. $U_{xm}(x)\cos m\psi$ is the longitudinal mode shape function; $U_{\psi m}(x)\sin m\psi$ is the circumferential mode shape function; and $U_{3m}(x)\cos m\psi$ is the transverse mode shape function. Thus, the modal forces induced by distributed mechanical loading (i.e., external forces) and the distributed actuator (i.e., control forces) become

$$\begin{aligned}\hat{F}_m = \frac{1}{\rho h N_m}\int_x\int_\psi \{&F_x[U_{xm}(x)\cos(m\psi)] + F_\psi[U_{\psi m}(x)\sin(m\psi)]\\ &+ F_3[U_{3m}(x)\cos(m\psi)]\}x\,\sin\,\beta^*\,\mathrm{d}x\,\mathrm{d}\psi,\end{aligned} \tag{12}$$

$$\begin{aligned}\hat{F}^c_m = \frac{1}{\rho h N_m}\int_x\int_\psi \Bigg\{&-\left\{\frac{\partial N^c_{xx}}{\partial x} + \frac{1}{x}(N^c_{xx} - N^c_{\psi\psi})\right\}U_{xm}(x)\cos(m\psi)\\ &- \frac{1}{x\,\sin\,\beta^*}\left\{\frac{\partial N^c_{\psi\psi}}{\partial\psi} + \frac{1}{x\,\tan\,\beta^*}\frac{\partial M^c_{\psi\psi}}{\partial\psi}\right\}U_{\psi m}(x)\sin(m\psi)\\ &- \left\{\frac{2}{x}\frac{\partial M^c_{xx}}{\partial x} + \frac{\partial^2 M^c_{xx}}{\partial x^2} - \frac{1}{x}\frac{\partial M^c_{\psi\psi}}{\partial x} + \frac{1}{x^2\sin^2\beta^*}\frac{\partial^2 M^c_{\psi\psi}}{\partial\psi^2} - \frac{N^c_{\psi\psi}}{x\,\tan\,\beta^*}\right\}\\ &\times U_{3m}(x)\cos(m\psi)\Bigg\}x\,\sin\,\beta^*\,\mathrm{d}x\,\mathrm{d}\psi\end{aligned} \tag{13}$$

and

$$N_m = \int_x\int_\psi\left\{\left[\left(\frac{x}{x_2}\right)^p\cos\,m\psi\right]^2 + \left[\left(\frac{x}{x_2}\right)^p\sin\,m\psi\right]^2 + \left[\left(\frac{x}{x_2}\right)^p\cos\,m\psi\right]^2\right\}x\,\sin\,\beta^*\,\mathrm{d}x\,\mathrm{d}\psi. \tag{14}$$

Detailed distributed control forces and moments induced by distributed actuators are further defined next.

3. Distributed micro-control characteristics

The control forces and moments induced by the piezoelectric actuator with an applied voltage ϕ^a are given as [11]

$$N^c_{xx} = d_{31}Y_p\phi^a, \tag{15}$$

$$N^c_{\psi\psi} = d_{32}Y_p\phi^{\mathrm{a}}, \tag{16}$$

$$M^c_{xx} = r^a_x d_{31}Y_p\phi^a, \tag{17}$$

$$M^c_{\psi\psi} = r^a_\psi d_{32}Y_p\phi^a. \tag{18}$$

Substituting actuator induced forces and moments into the generic modal control force expression $\hat{F}^c_m$ and separating them into individual contributing microscopic membrane/bending control actions gives

$$(\hat{T}_m)_{x,\mathrm{mem}} = \frac{d_{31}Y_p}{\rho h N_m}\int_x\int_\psi\left\{\left(-\frac{\partial\phi^a}{\partial x} - \frac{\phi^a}{x}\right)U_{xm}(x)\cos(m\psi)\right\}x\,\sin\,\beta^*\,\mathrm{d}x\,\mathrm{d}\psi, \tag{19}$$

$$(\hat{T}_m)_{\psi,\text{mem}} = \frac{d_{32}Y_p}{\rho h N_m}\int_x\int_\psi\left\{\frac{1}{x}\phi^{\text{a}}U_{xm}(x)\cos(m\psi) - \frac{1}{x\sin\beta^*}\left(\frac{\partial\phi^a}{\partial\psi}\right)\right.$$
$$\left.\times\, U_{\psi m}(x)\sin(m\psi) + \frac{\phi^a}{x\tan\beta^*}U_{3m}(x)\cos(m\psi)\right\}x\sin\beta^*\,\mathrm{d}x\,\mathrm{d}\psi. \tag{20}$$

$$(\hat{T}_m)_{x,\text{bend}} = \frac{r_x^a d_{31}Y_p}{\rho h N_m}\int_x\int_\psi\left\{\left[-\frac{2}{x}\frac{\partial\phi^a}{\partial x} - \frac{\partial^2\phi^a}{\partial x^2}\right]U_{3m}(x)\cos(m\psi)\right\}x\sin\beta^*\,\mathrm{d}x\,\mathrm{d}\psi, \tag{21}$$

$$(\hat{T}_m)_{\psi,\text{bend}} = \frac{r_\psi^a d_{32}Y_p}{\rho h N_m}\int_x\int_\psi\left\{\left[-\frac{\cos\beta^*}{x^2\sin^2\beta^*}\frac{\partial\phi^a}{\partial\psi}\right]U_{\psi m}(x)\sin(m\psi)\right.$$
$$\left.+\left[\frac{1}{x}\frac{\partial\phi^a}{\partial x} - \frac{1}{x^2\sin^2\beta^*}\frac{\partial^2\phi^a}{\partial\psi^2}\right]U_{3m}(x)\cos(m\psi)\right\}x\sin\beta^*\,\mathrm{d}x\,\mathrm{d}\psi. \tag{22}$$

Note that $(\hat{T}_m)_{x,\text{mem}}$ is the membrane force component in the x direction, $(\hat{T}_m)_{\psi,\text{mem}}$ is the membrane force component in the ψ direction, $(\hat{T}_m)_{x,\text{bend}}$ is the bending force component in the x direction, and $(\hat{T}_m)_{\psi,\text{bend}}$ is the bending force component in the ψ direction. Assume the piezoelectric actuator is hexagonal structure ($C_{6v} = 6\,\text{mm}$) i.e., $d_{32} = d_{31}$, with uniform thickness; and recall that the conical shell has constant thickness also. Thus, the distances measured from the shell neutral surface to the actuator mid-surface are $r_x^a = r_\psi^a = r^a$. The micro-control actions defined in Eqs. (19)–(22) now become

$$(\hat{T}_m)_{x,\text{mem}} = \frac{d_{31}Y_p}{\rho h N_m}\int_x\int_\psi\left\{\left(-\frac{\partial\phi^a}{\partial x} - \frac{\phi^a}{x}\right)U_{xm}(x)\cos(m\psi)\right\}x\sin\beta^*\,\mathrm{d}x\,\mathrm{d}\psi, \tag{23}$$

$$(\hat{T}_m)_{\psi,\text{mem}} = \frac{d_{31}Y_p}{\rho h N_m}\int_x\int_\psi\left\{\frac{1}{x}\phi^a U_{xm}(x)\cos(m\psi) - \frac{1}{x\sin\beta^*}\left(\frac{\partial\phi^a}{\partial\psi}\right)\right.$$
$$\left.\times\, U_{\psi m}(x)\sin(m\psi) + \frac{\phi^{\text{a}}}{x\tan\beta^*}U_{3m}(x)\cos(m\psi)\right\}x\sin\beta^*\,\mathrm{d}x\,\mathrm{d}\psi, \tag{24}$$

$$(\hat{T}_m)_{x,\text{bend}} = \frac{r^a d_{31}Y_p}{\rho h N_m}\int_x\int_\psi\left\{\left[-\frac{2}{x}\frac{\partial\phi^a}{\partial x} - \frac{\partial^2\phi^a}{\partial x^2}\right]U_{3m}(x)\cos(m\psi)\right\}x\sin\beta^*\,\mathrm{d}x\,\mathrm{d}\psi, \tag{25}$$

$$(\hat{T}_m)_{\psi,\text{bend}} = \frac{r^a d_{31}Y_p}{\rho h N_m}\int_x\int_\psi\left\{\left[-\frac{\cos\beta^*}{x^2\sin^2\beta^*}\frac{\partial\phi^a}{\partial\psi}\right]U_{\psi m}(x)\sin(m\psi)\right.$$
$$\left.+\left[\frac{1}{x}\frac{\partial\phi^a}{\partial x} - \frac{1}{x^2\sin^2\beta^*}\frac{\partial^2\phi^a}{\partial\psi^2}\right]U_{3m}(x)\cos(m\psi)\right\}x\sin\beta^*\,\mathrm{d}x\,\mathrm{d}\psi. \tag{26}$$

Thus, the generic control force $\hat{F}_m^c$ can be explicitly defined by its four contributing micro-control actions, i.e.,

$$\hat{F}_m^c = (\hat{T}_m)_{x,\text{mem}} + (\hat{T}_m)_{\psi,\text{mem}} + (\hat{T}_m)_{x,\text{bend}} + (\hat{T}_m)_{\psi,\text{bend}}. \tag{27}$$

4. Micro-control actions of patch actuators

Note that $F_m = \hat{F}_m + \hat{F}_m^c$ and the mechanical input $\hat{F}_m$ is neglected in the control action analysis. The transverse actuating voltages $\phi^a(x,\psi,t)$ applied to an actuator patch defined from x_1^* to x_2^* in the longitudinal direction and ψ_1^* to ψ_2^* in the circumferential direction can be expressed by a time dependent part and a spatial distribution part

$$\phi^a(x,\psi,t) = \phi^a(t)[u_s(x-x_1^*) - u_s(x-x_2^*)][u_s(\psi-\psi_1^*) - u_s(\psi-\psi_2^*)], \tag{28}$$

where $u_s(\cdot)$ is the unit step function: $u_s(\psi-\psi_i^*)=1$ when $\psi\geqslant\psi_i^*$, and $=0$ when $\psi<\psi_i^*$. Thus, the spatial derivatives of the transverse actuating signals in Eqs. (23)–(26) are

$$\frac{\partial}{\partial x}\phi^a(x,\psi,t)=\phi^a(t)[\delta(x-x_1^*)-\delta(x-x_2^*)][u_s(\psi-\psi_1^*)-u_s(\psi-\psi_2^*)], \tag{29}$$

$$\frac{\partial}{\partial \psi}\phi^a(x,\psi,t)=\phi^a(t)[u_s(x-x_1^*)-u_s(x-x_2^*)][\delta(\psi-\psi_1^*)-\delta(\psi-\psi_2^*)], \tag{30}$$

where $\delta(\cdot)$ is a Dirac delta function: $\int\delta(\psi-\psi_i^*)\,\mathrm{d}\psi=1$ when $\psi=\psi_i^*$, and $=0$ when $\psi\neq\psi_i^*$. Thus, the micro-control actions restricted by the segmented electrode on the segmented actuator can be further explicitly defined accordingly. Substituting the patch definition and further manipulating the four micro-control actions yields

$$(\hat{T}_m)_{x,\mathrm{mem}}=-\frac{d_{31}Y_p\phi^a(t)\sin\beta^*}{\rho hN_m}\int_x\{[x[\delta(x-x_1^*)-\delta(x-x_2^*)]+1]U_{xm}(x)\}\,\mathrm{d}x\times\int_\psi\cos(m\psi)\,\mathrm{d}\psi, \tag{31}$$

$$(\hat{T}_m)_{\psi,\mathrm{mem}}=\frac{d_{31}Y_p\phi^a(t)}{\rho hN_m}\left\{\sin\beta^*\int_x U_{xm}(x)\,\mathrm{d}x\int_\psi\cos(m\psi)\,\mathrm{d}\psi-\int_\psi[\delta(\psi-\psi_1^*)-\delta(\psi-\psi_2^*)]\sin(m\psi)\,\mathrm{d}\psi\int_x U_{\psi m}(x)\,\mathrm{d}x+\cos\beta^*\int_x U_{3m}(x)\,\mathrm{d}x\int_\psi\cos(m\psi)\,\mathrm{d}\psi\right\}, \tag{32}$$

$$(\hat{T}_m)_{x,\mathrm{bend}}=\frac{r^a d_{31}Y_p\phi^a(t)\sin\beta^*}{\rho hN_m}\left\{\int_x[-2[\delta(x-x_1^*)-\delta(x-x_2^*)]-x\frac{\partial}{\partial x}[\delta(x-x_1^*)-\delta(x-x_2^*)]]U_{3m}(x)\,\mathrm{d}x\int_\psi\cos(m\psi)\,\mathrm{d}\psi\right\}, \tag{33}$$

$$(\hat{T}_m)_{\psi,\mathrm{bend}}=\frac{r^a d_{31}Y_p\phi^a(t)}{\rho hN_m}\left\{-\frac{1}{\tan\beta^*}\int_x\frac{U_{\psi m}(x)}{x}\,\mathrm{d}x\int_\psi[\delta(\psi-\psi_1^*)-\delta(\psi-\psi_2^*)]\times\sin(m\psi)\,\mathrm{d}\psi+\sin\beta^*\int_x U_{3m}(x)[\delta(x-x_1^*)-\delta(x-x_2^*)]\,\mathrm{d}x\int_\psi\cos(m\psi)\,\mathrm{d}\psi-\frac{1}{\sin\beta^*}\int_x\frac{U_{3m}(x)}{x}\,\mathrm{d}x\int_\psi\frac{\partial}{\partial\psi}[(\psi-\psi_1^*)-\delta(\psi-\psi_2^*)]]\cos(m\psi)\,\mathrm{d}\psi\right\}. \tag{34}$$

These four equations represent directional modal micro-control characteristics of distributed patch actuators laminated on a conical shell. Detailed micro-control characteristics are presented in case studies next.

5. Parametric studies of micro-control actions

To keep the generality, material parameters, e.g., d_{31}, d_{32}, Y_p and ρ, are assumed unity when evaluating the micro-control actions of conical shell sections. Thus, manipulating these parameters (e.g., $(r^a d_{3i}Y_p)/\rho$), one can further extrapolate analysis data and evaluate control characteristics of specific actuator materials and natural modes. Note that the control signal $\phi^a(t)$ is assumed unity for all cases also. Thus, the segmented actuator patches would reveal the true inherent actuator characteristics and micro-control actions. Dimensions of the truncated conical shell model are: major edge radius $R=0.154\,\mathrm{m}$ (6.07 in), minor edge radius $r=0.069\,\mathrm{m}$ (2.72 in), semi-vertex angle $=14.24^\circ$ (0.248535 rad), shell thickness $h=0.000254\,\mathrm{m}$ (0.01 in), actuator placement at $r^a=0.000127\,\mathrm{m}$ (0.005 in), and length $L=0.33528\,\mathrm{m}$ (13.2 in). The conical shell has free boundary conditions at the top and bottom ends, Fig. 2. Note that the actuator patch is assumed thin, such that its elastic effect is neglected. Piezoelectric actuator patches with an area of 15° in the circumferential direction (i.e., the first patch is from 0° to 15°, the next patch is from 15° to 30° and so on in the

ψ direction), and 0.02894 m in the longitudinal direction are laminated throughout the conical shell section, Fig. 2. Note that although all actuation characteristics of a full-revolution truncated conical shell are calculated, control actions related to a half of the revolution (i.e., $\psi = \pi$) are presented later.

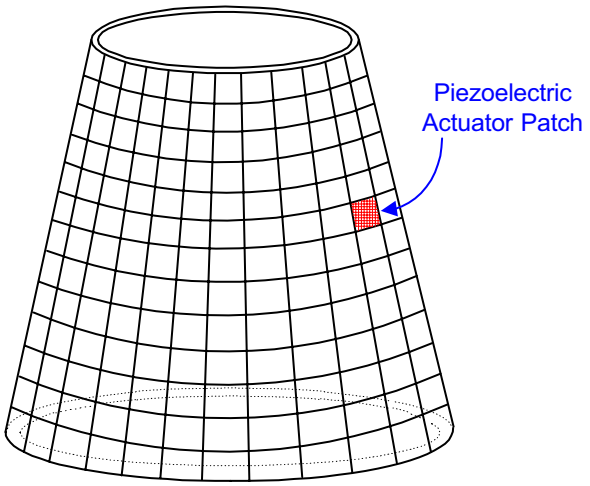

Fig. 2. A conical shell laminated with piezoelectric actuator patches.

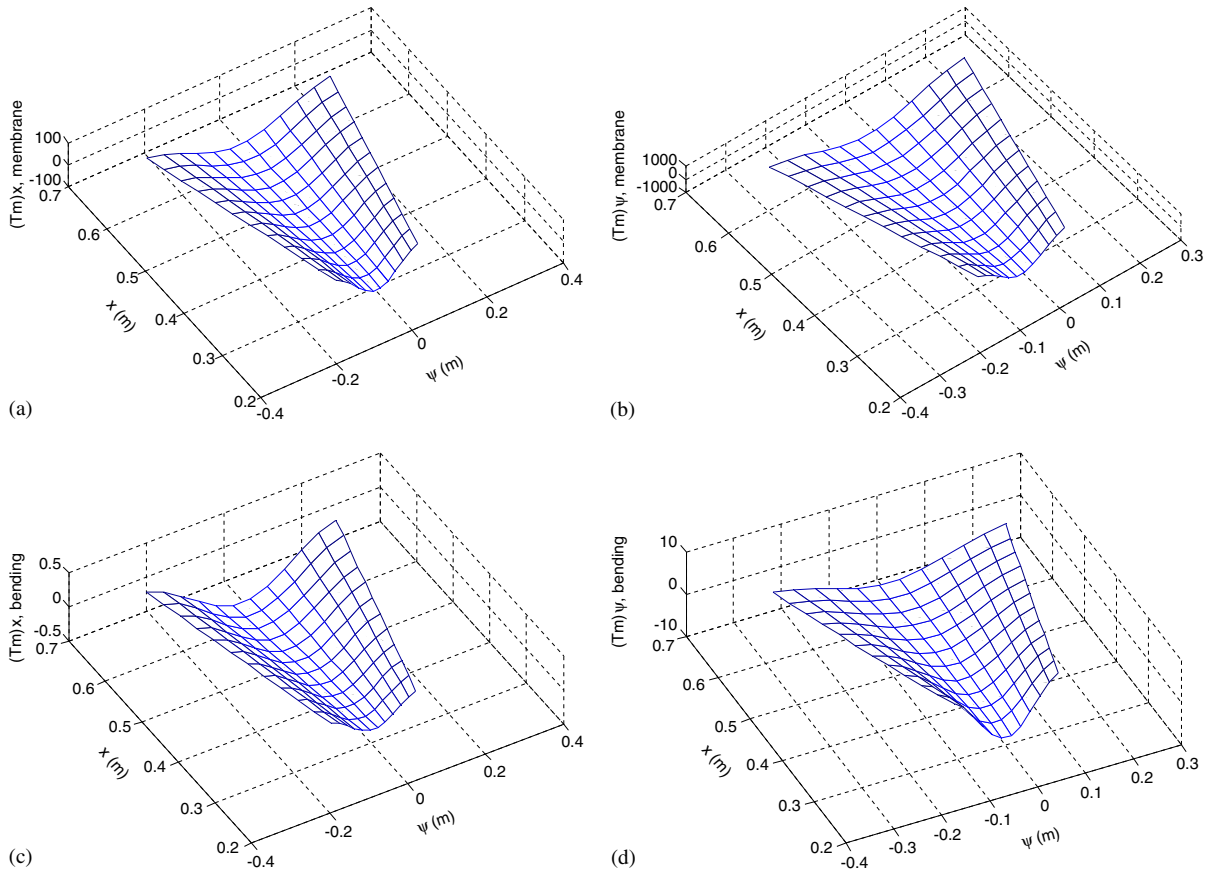

Fig. 3. Micro-control actions of the (1,2) conical shell mode: (a) Longitudinal membrane actuation$(\hat{T}_m)_{x,\mathrm{mem}}$; (b) circumferential membrane actuation $(\hat{T}_m)_{\psi,\mathrm{mem}}$; (c) longitudinal bending actuation $(\hat{T}_m)_{x,\mathrm{bend}}$; (d) circumferential bending actuation:$(\hat{T}_m)_{\psi,\mathrm{bend}}$.

Recall that $(\hat{T}_m)_{x,\text{mem}}$ is the longitudinal micro-membrane control force component, $(\hat{T}_m)_{\psi,\text{mem}}$ is the circumferential membrane control force component, $(\hat{T}_m)_{x,\text{bend}}$ is the longitudinal bending control component, and $(\hat{T}_m)_{\psi,\text{bend}}$ is the circumferential bending control component. These actuator induced micro-control actions of the conical shell modes, i.e., 1st and 2nd x-mode group with $m = 2, \ldots, 5$ are analyzed and grouped. Recall that m denotes the circumferential wavenumber. Each data point (or magnitude) on the graph represents the micro-control action of a segmented actuator patch at the corresponding location of the conical shell section. Connecting these microscopic actuations provides a global spatial distribution of actuation forces of each shell mode.

5.1. *Mode group 1:* ($p = 1$, $m = 2 - 5$) *modes*

For the first mode group (i.e., $(x/x_2)^p$ with $p = 1$) of the conical shell section, $U_{xm}(x)$, $U_{\psi m}(x)$ and $U_{3m}(x)$ are (x/x_2) [9]. Detailed longitudinal and circumferential membrane/bending micro-control actions of actuator patches laminated at various locations are plotted in Figs. 3–6 where $m = 2-5$ of the 1st mode group, i.e., $(1,m = 2-5)$. Note that there are four components in each figure, i.e.: (a) longitudinal membrane actuation $(\hat{T}_m)_{x,\text{mem}}$; (b) circumferential membrane actuation $(\hat{T}_m)_{\psi,\text{mem}}$; (c) longitudinal bending actuation $(\hat{T}_m)_{x,\text{bend}}$; (d) circumferential bending actuation $(\hat{T}_m)_{\psi,\text{bend}}$. To illustrate the prospective view of the conical shell in micro-actuation characteristics, the half-conical shell section remains in the original aspect ratio and both longitudinal and circumferential dimensions (in meter) are used in these figures.

5.2. *Mode group 2:* ($p = 2$, $m = 2 - 5$) *modes*

For the second mode group (i.e., $(x/x_2)^p$ with $p = 2$) of the conical shell section, $U_{xm}(x)$, $U_{\psi m}(x)$ and $U_{3m}(x)$ are $(x/x_2)^2$ [9]. Detailed longitudinal and circumferential membrane/bending micro-control actions are plotted in Figs. 7–10 where $m = 2-5$ of the 2nd mode group, i.e., $(2, m = 2–5)$. Again, there are four components in

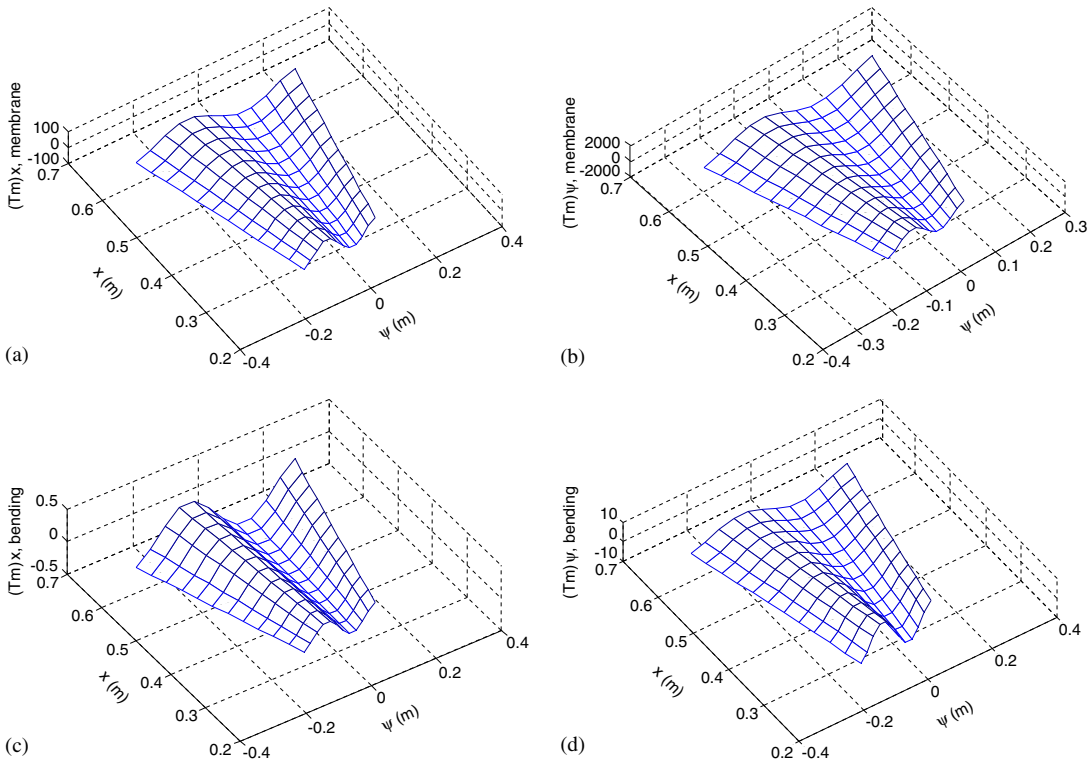

Fig. 4. Micro-control actions of the (1,3) conical shell mode.

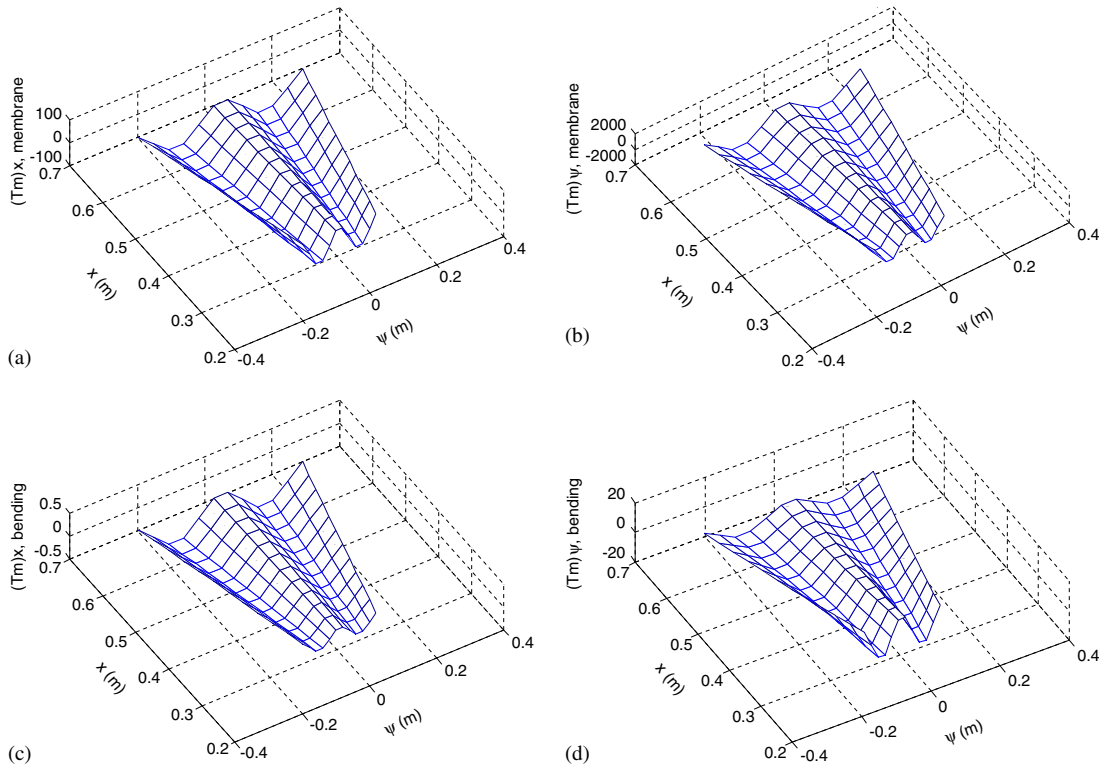

Fig. 5. Micro-control actions of the (1,4) conical shell mode.

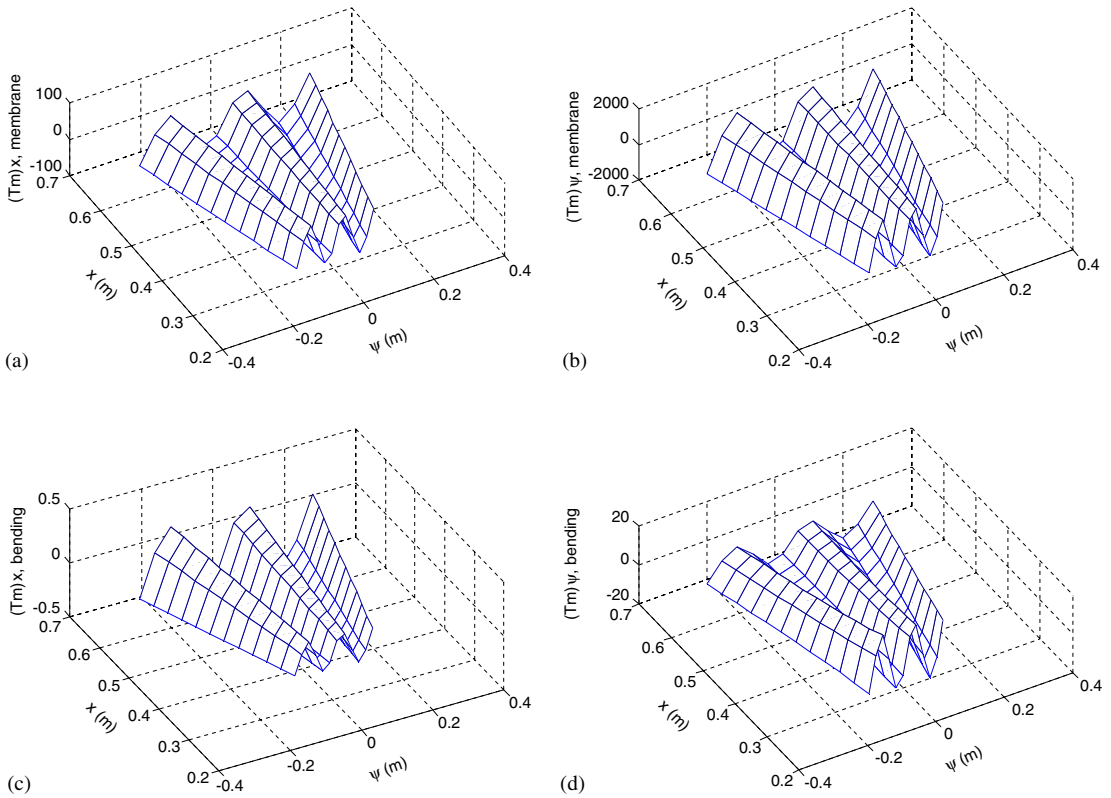

Fig. 6. Micro-control actions of the (1,5) conical shell mode.

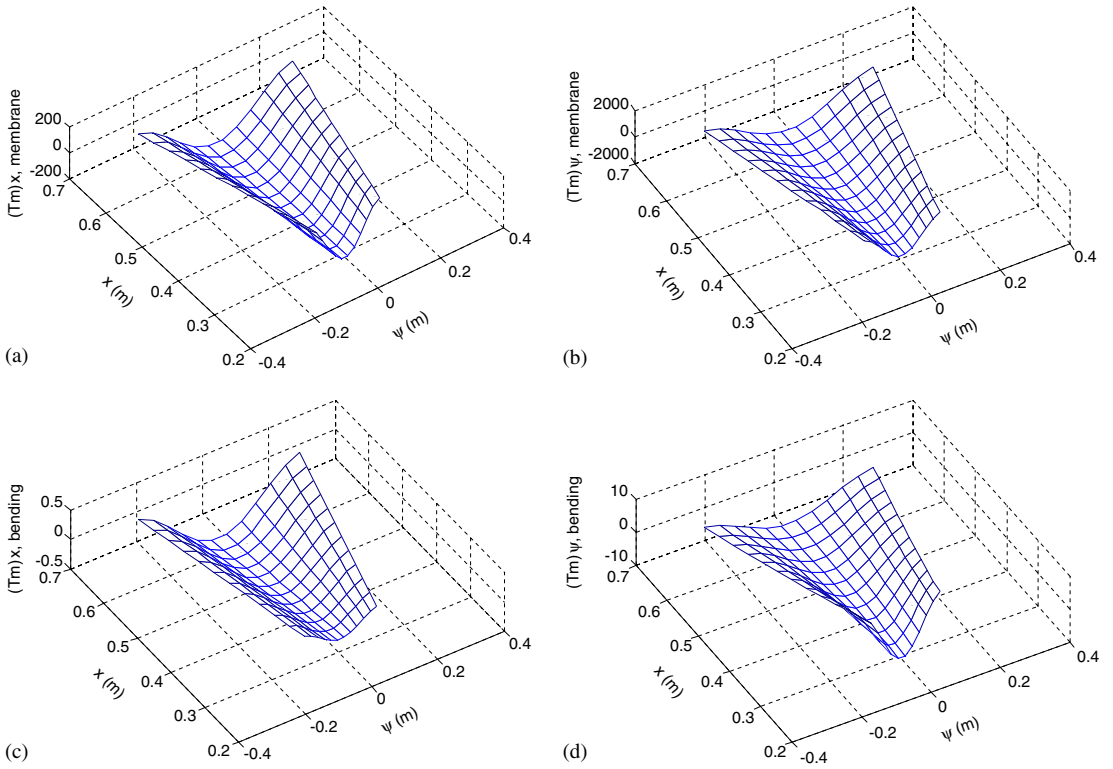

Fig. 7. Micro-control actions of the (2,2) conical shell mode: (a) longitudinal membrane actuation$(\hat{T}_m)_{x,\mathrm{mem}}$; (b) circumferential membrane actuation $(\hat{T}_m)_{\psi,\mathrm{mem}}$; (c) longitudinal bending actuation $(\hat{T}_m)_{x,\mathrm{bend}}$; (d) circumferential bending actuation:$(\hat{T}_m)_{\psi,\mathrm{bend}}$.

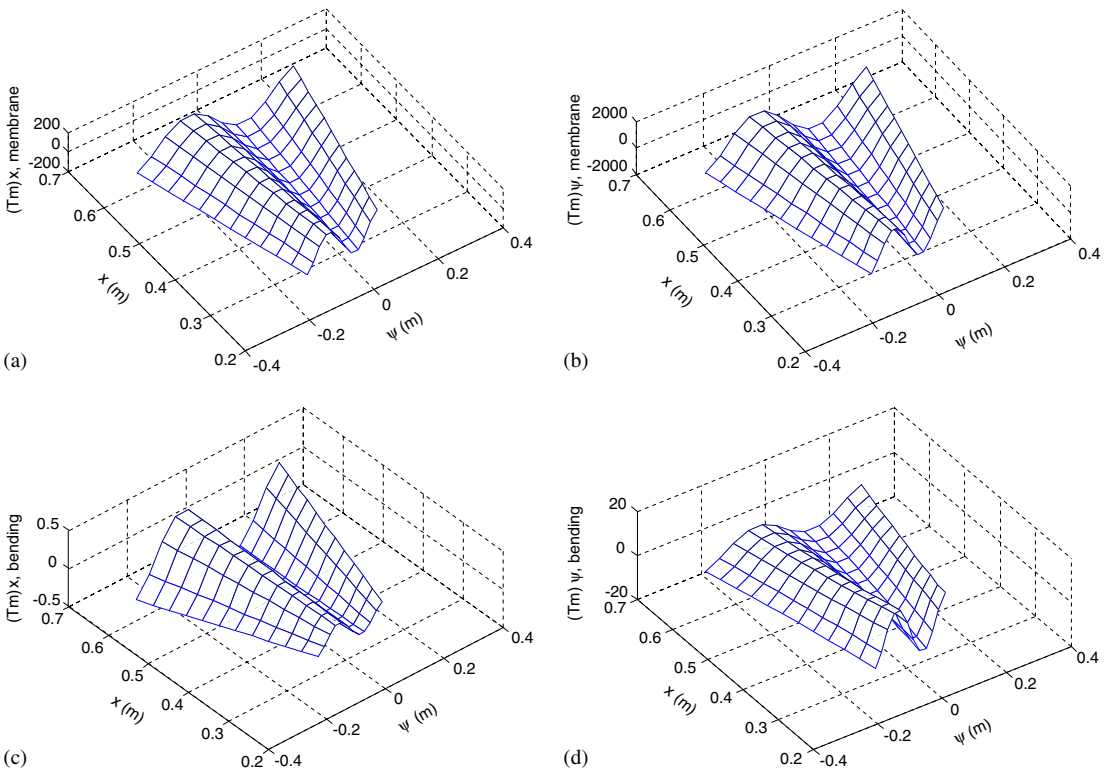

Fig. 8. Micro-control actions of the (2,3) conical shell mode.

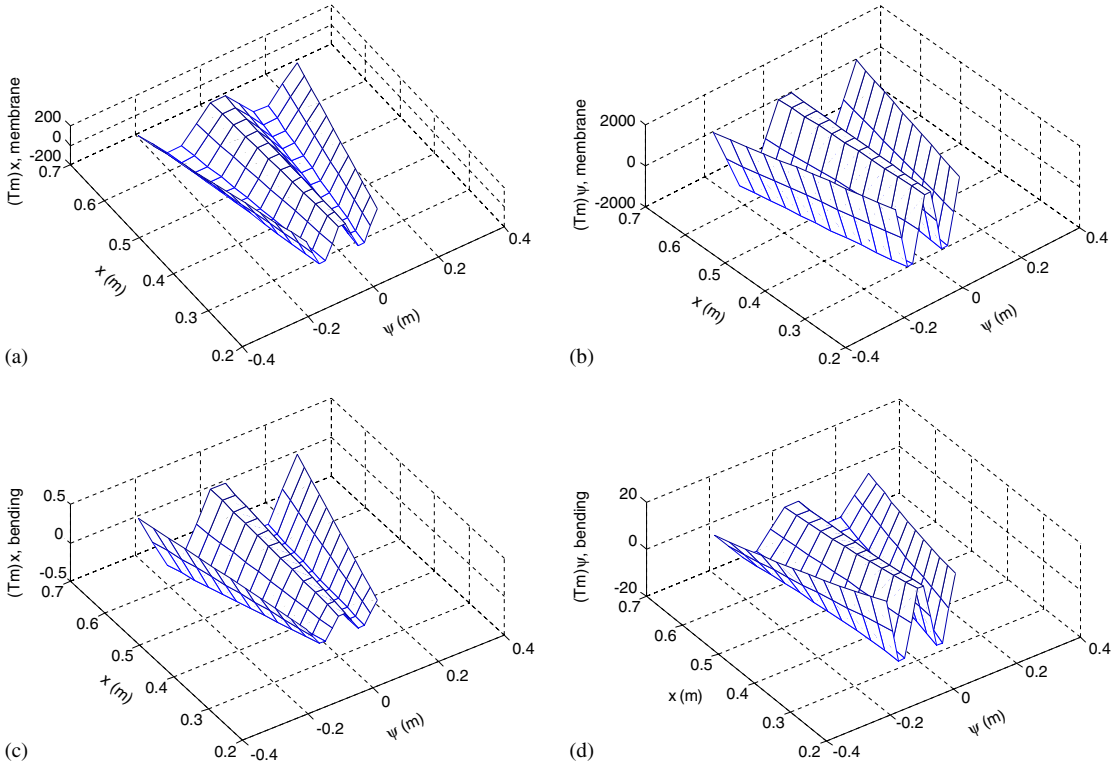

Fig. 9. Micro-control actions of the (2,4) conical shell mode.

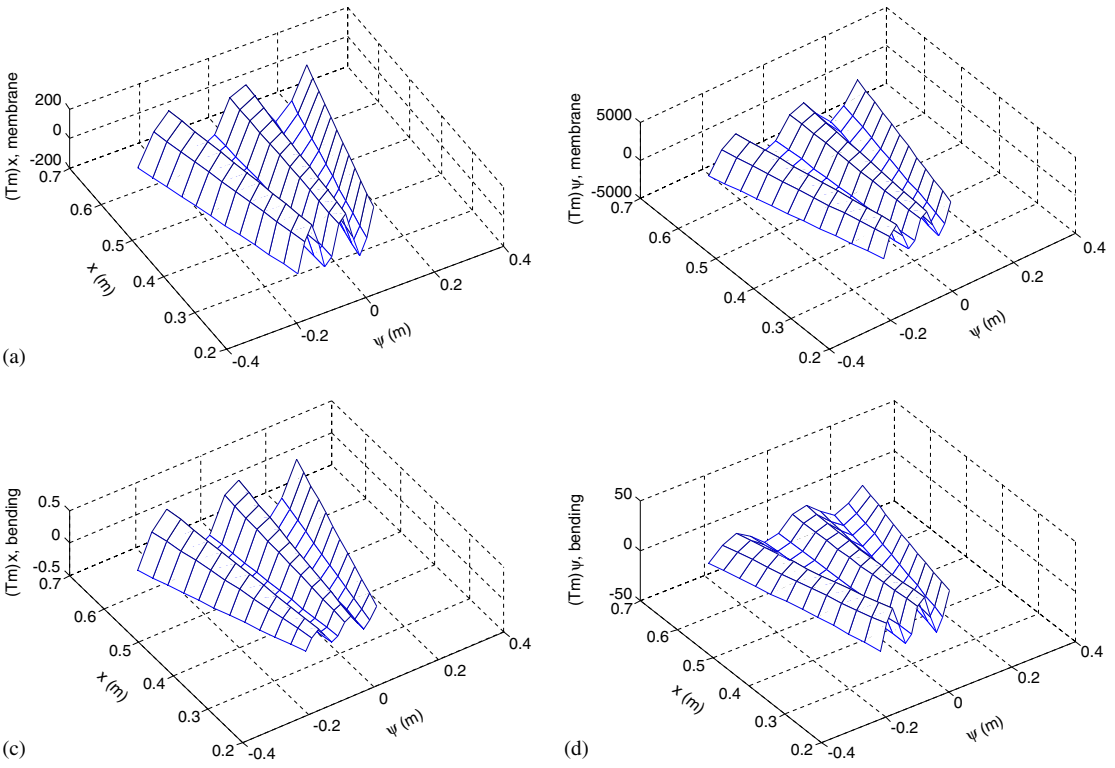

Fig. 10. Micro-control actions of the (2,5) conical shell mode.

each figure, i.e.: (a) longitudinal membrane actuation $(\hat{T}_m)_{x,\text{mem}}$; (b) circumferential membrane actuation $(\hat{T}_m)_{\psi,\text{mem}}$; (c) longitudinal bending actuation $(\hat{T}_m)_{x,\text{bend}}$; (d) circumferential bending actuation $(\hat{T}_m)_{\psi,\text{bend}}$.

The micro-control actions of the (1, $m = 2-5$) and (2, $m = 2-5$) conical shell modes reveal that the magnitudes of micro-control actions are $(\hat{T}_m)_{\psi,\text{mem}} \gg (\hat{T}_m)_{x,\text{mem}} \gg (\hat{T}_m)_{\psi,\text{bend}} \gg (\hat{T}_m)_{x,\text{bend}}$. $(\hat{T}_m)_{\psi,\text{mem}}$ dominates and $(\hat{T}_m)_{x,\text{bend}}$ is almost negligible in the total control force. Moreover, the analyses show that $(\hat{T}_m)_{x,\text{mem}}$ and $(\hat{T}_m)_{x,\text{bend}}$ remain about the same order of magnitude when circumferential mode m changes from 2 to 5. $(\hat{T}_m)_{\psi,\text{mem}}$ and $(\hat{T}_m)_{\psi,\text{bend}}$ actions increase at higher circumferential mode number. $(\hat{T}_m)_{\psi,\text{mem}}$ is larger than $(\hat{T}_m)_{x,\text{mem}}$, ranging from 2 to 20 times depending on modes. Detailed data also reveal that the micro-control action at the minor-end of the conical shell is relatively high as compared with that at the major-end of the shell section, see Eq. (34).

6. Conclusions

Distributed precision control of conical shell sections is a critical issue in high-performance structural systems, e.g., rocket fairings, turbines, load-carrying structures of solid rocket motor cases, etc. This study is to evaluate microscopic actuation characteristics and control actions of segmented actuator patches laminated on flexible conical shells. Mathematical models and modal domain governing equations of the conical shell section laminated with distributed actuator patches were presented first, followed by formulation of distributed control forces and micro-control actions including longitudinal/circumferential membrane and bending control components. The mode shape functions of the conical shell section with free–free boundary conditions are based on the Donnell–Mushtari–Vlasov theory. These mode shape functions were used in the modal control force expression and the micro-control action analyses. Spatially distributed electromechanical actuation characteristics contributed by various longitudinal/circumferential membrane and bending control actions were investigated. Distributed control forces and micro actions of actuator patches at various locations were analyzed and its modal-dependent spatial control effectives evaluated.

Analysis data show that, for conical shell mode (1, $m = 2-5$) and (2, $m = 2-5$), the circumferential micro-control action $(\hat{T}_m)_{\psi,\text{mem}}$ dominants as compared with the other three modal control actions and it is followed by $(\hat{T}_m)_{x,\text{mem}}$, $(\hat{T}_m)_{\psi,\text{bend}}$ and $(\hat{T}_m)_{x,\text{bend}}$ control actions in both cases. Note that the control signal $\phi^a(t)$ and other material parameters $(r^a d_{3i} Y_p)/\rho$ were assumed unity for all cases, thus the segmented actuator patches would reveal the true inherent actuator characteristics and micro-control actions. Specific spatial control behavior can be explicitly defined once these parameters are identified. Furthermore, the magnitudes of control forces and micro-control actions are modal dependent. Referring to these data, one can effectively configure actuator placements to achieve the maximal control effectiveness at minimal actuator power or size requirements.

Acknowledgments

This research is supported, in part, by a Grant (F49620-98-1-0467) from the Air Force Office of Scientific Research (Project Manager: Brian Sanders). This support is gratefully acknowledged.

References

[1] W.C.L. Hu, Free vibration of conical shells, *NASA Report TN D-2666*, 1964.
[2] W.C.L. Hu, J.F. Gormley, U.S. Lindholm, Flexural vibrations of conical shells with free edges, *NASA Report CR* 384 (1966) 0.
[3] F.A. Krause, Natural frequencies and mode shapes of the truncated conical shell with edges, Ph.D. Dissertation, The University of Arizona, 1968.
[4] L. Tong, Effect of axial load on free vibration of orthotropic truncated conical shells, *ASME Transaction, Journal of Vibration and Acoustics* 118 (1996) 164–168.
[5] C.W. Lim, K.M. Liew, Vibratory behavior of shallow conical shells by a global Ritz formulation, *Engineering Structures* 17 (1995) 63–70.
[6] K.M. Liew, C.W. Lim, S. Kitipornchai, Vibration of shallow shells: a review with bibliography, *Applied Mechanics Reviews* 50 (1997) 431–444.

[7] K.M. Liew, Z.C. Feng, Vibration characteristics of conical shell panels with three-dimensional flexibility, *ASME Transaction, Journal of Applied Mechanics* 67 (1997) 314–320.
[8] U. Gabbert, H.S. Tzou (Eds.), *Smart Structures and Structronic Systems*, Kluwer Academic Publishers, Boston/Dordrecht, 2001.
[9] H.S. Tzou, D.W. Wang, W.K. Chai, Dynamics and distributed control of conical shell laminated with full and diagonal actuators, *Journal of Sound and Vibration* 256 (2001) 65–79.
[10] K.M. Liew, X.Q. He, T.Y. Ng, S. Kitipornchai, Active control of FGM shells subjected to a temperature gradient via piezoelectric sensor/actuator patches, *International Journal for Numerical Methods in Engineering* 55 (2002) 653–668.
[11] H.S. Tzou, J.H. Ding, I. Hagiwara, Micro-control actions of distributed actuators laminated on precision paraboloidal structronics shells, *JSME International Journal, Series C* 45 (2002) 8–15.
[12] R. Howard, W.K. Chai., H.S. Tzou, Modal voltages of linear and non linear structures using distributed artificial neurons, *Mechanical Systems and Signal Processing* 15 (2001) 629–640.
[13] H.S. Tzou, W.K. Chai, D.W. Wang, Modal voltages and distributed signal analysis of conical shells of revolution, *Journal of Sound and Vibration* 260 (2003) 589–609.
[14] W.K. Chai, P. Smithmaitrie, H.S. Tzou, Neural potentials and micro signals of nonlinear deep and shallow conical shells, *Mechanical Systems and Signal Processing* 18 (2003) 959–975.
[15] H.S. Tzou, *Piezoelectric Shells—Distributed Sensing and Control of Continua*, Kluwer Academic Publishers, Boston/Dordrecht, 1993.